

Scattering of Neutrons from ^{16}O in the 2.2- to 4.2-MeV Energy Range*

C. H. JOHNSON AND J. L. FOWLER
Oak Ridge National Laboratory, Oak Ridge, Tennessee
 (Received 7 April 1967)

We have measured the differential cross sections for scattering of neutrons from ^{16}O at some 14 energies between 2.2- and 4.2-MeV neutron energy by detecting scattered neutrons. In the vicinity of the 3.77-MeV peak in the total cross section of ^{16}O , we redetermined the total cross section with a 5-keV energy spread. From a phase-shift analysis of our data and other data taken from the literature, we assign resonance parameters for seven states of ^{17}O between 7.30- and 8.21-MeV excitation energy as follows (in order: excitation energy of ^{17}O , J value, parity, and reduced width in single-particle units, $\hbar^2/\mu a^2$): 7.30 ($\frac{3}{2}^+$, 0.23), 7.67 ($\frac{3}{2}^-$, 0.07), 7.691 ($\frac{3}{2}^-$, 0.03), 7.694 ($\frac{3}{2}^+$, 0.001), 7.91 ($\frac{3}{2}^-$, 0.02), 8.08 ($\frac{3}{2}^+$, 0.03), and 8.21 ($\frac{3}{2}^-$, 0.01). Our finding the narrow $\frac{3}{2}^+$ state at 7.694 MeV has removed a difficulty in resonance-parameter assignment at the 3.77-MeV neutron energy peak in the total cross section of ^{16}O .

I. INTRODUCTION

IN first approximation, nuclei which are one nucleon beyond a closed shell should show simple single-particle states. Indeed, the low-lying even-parity states of ^{17}O and ^{17}F do have a great deal of single-particle character. Nevertheless, there are many odd-parity states at low energies as well as even-parity states at higher energies for which an explanation must consider excitations of the doubly closed-shell ^{16}O core. The advent of electronic computers, together with the development of means of handling the nuclear many-body problem, offers the opportunity for understanding these excitations. In fact, there has been recently a great deal of theoretical interest, as well as some success, in the explanation of the spectroscopy of the mass-17 nuclei.¹⁻³ In spite of this interest and the obvious importance of the mass-17 nuclei, there have remained conspicuous gaps in the experimental knowledge of their spectroscopy. Possibly because scattering of protons by ^{16}O is easier than scattering of neutrons by this nucleus, the experimental situation⁴⁻⁹ with regard to ^{17}F has been in a somewhat better condition than that for ^{17}O . In the latter case, only recently has there been an intensive effort to unravel the resonance structure at neutron scattering energies between 2 and 4 MeV in terms of J values, parities, and widths of the observed resonances. Some total-neutron-cross-section measurements^{10,11} and results from the study of the $^{13}\text{C}(\alpha, n)^{16}\text{O}$

reaction¹²⁻¹⁶ have located the principal resonances in this energy region and have allowed certain J value assignments. These, coupled with an earlier low-resolution differential cross-section experiment,¹⁷ have also led to the identification of the parity of a few of the wide resonances. Recently, better energy resolution differential cross-section measurements at the Oak Ridge National Laboratory¹⁸ and at Columbia University¹⁹ have removed most of the difficulties with regard to the detailed resonance parameter assignments in the 2.2-4.3-MeV neutron energy range.

In this paper we shall discuss our accumulated measurements of differential scattering cross sections between 2.2 and 4.2 MeV and the phase-shift analysis of these together with other differential cross sections which have appeared in the literature.²⁰ We shall present new information and analyses which resolve a difficulty that had arisen in connection with the identification of an ~ 20 -keV wide peak at 3.77-MeV neutron scattering energy.^{10,11,18,19} In conclusion, we shall summarize the available experimental information on excited states of ^{17}O from zero up through 8.30 MeV with special emphasis on reduced widths in terms of the single-particle limits.

II. TOTAL CROSS SECTION

The ^{17}O state associated with the 3.77-MeV peak in ^{16}O neutron scattering corresponds closely, both in

¹¹ D. B. Fossan, R. L. Walter, W. E. Wilson, and H. H. Barschall, *Phys. Rev.* **123**, 209 (1961).

¹² T. W. Bonner, A. A. Kraus, J. B. Marion, and J. P. Schiffer, *Phys. Rev.* **102**, 1348 (1956).

¹³ M. G. Rusbridge, *Proc. Phys. Soc. (London)* **A69**, 830 (1956).

¹⁴ J. P. Schiffer, A. A. Kraus, and J. R. Risser, *Phys. Rev.* **105**, 1811 (1957).

¹⁵ R. B. Walton, J. D. Clement, and F. Boreli, *Phys. Rev.* **107**, 1065 (1957).

¹⁶ B. K. Barnes, T. A. Belote, and J. R. Risser, *Phys. Rev.* **140**, B616 (1965).

¹⁷ E. Baldinger, P. Huber, and W. G. Proctor, *Helv. Phys. Acta* **25**, 142 (1952).

¹⁸ J. L. Fowler and C. H. Johnson, *Bull. Am. Phys. Soc.* **10**, 261 (1965).

¹⁹ D. Lister and A. Sayres, *Phys. Rev.* **143**, 745 (1966); *Bull. Am. Phys. Soc.* **10**, 103 (1965).

²⁰ *Angular Distribution in Neutron-Induced Reactions*, edited by M. D. Goldberg, V. M. May, and J. R. Stehn, Brookhaven National Laboratory Report No. BNL-400, 2nd ed., Vol. I, 1962 (unpublished).

* Research sponsored by the U. S. Atomic Energy Commission under contract with the Union Carbide Corporation.

¹ S. Matthies, V. G. Neudachin, and Yu. F. Smirnov, *Nucl. Phys.* **38**, 63 (1962).

² G. E. Brown and A. M. Green, *Nucl. Phys.* **75**, 401 (1965).

³ B. Margolis and N. de Takacsy, *Can. J. Phys.* **44**, 1431 (1966).

⁴ R. A. Laubenstein and M. J. W. Laubenstein, *Phys. Rev.* **84**, 18 (1951).

⁵ F. Eppling, Ph. D. thesis, University of Wisconsin, 1952 (unpublished).

⁶ S. R. Salisbury, G. Hardie, L. Oppliger, and R. Dangle, *Phys. Rev.* **126**, 2143 (1962).

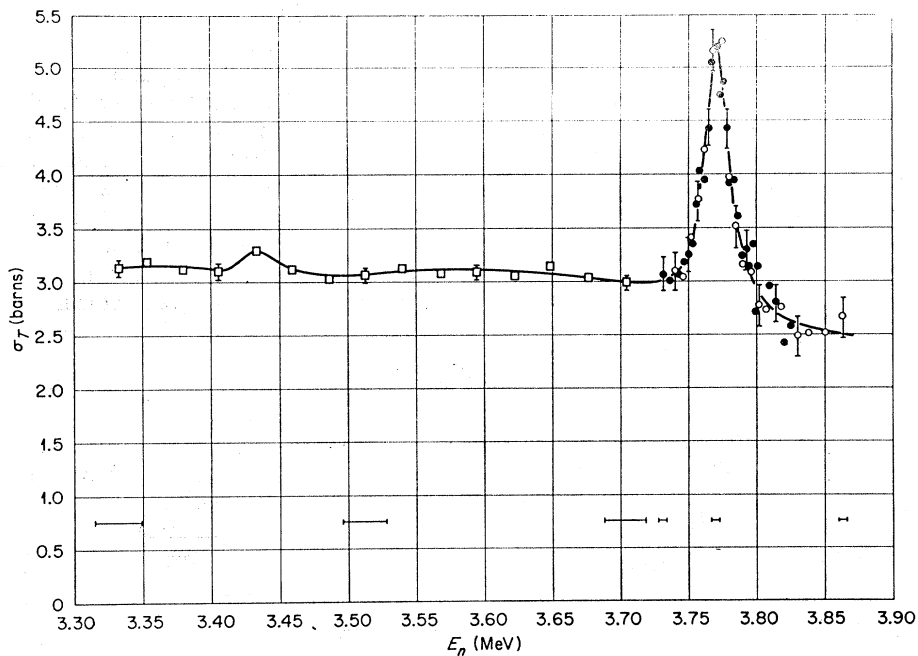
⁷ S. R. Salisbury and H. T. Richards, *Phys. Rev.* **126**, 2147 (1962).

⁸ R. W. Harris, G. C. Phillips, and C. M. Jones, *Nucl. Phys.* **38**, 259 (1962).

⁹ R. E. Segel, P. P. Singh, R. G. Allas, and S. S. Hanna, *Phys. Rev. Letters* **10**, 345 (1963).

¹⁰ K. Tsukada and T. Fuse, *J. Phys. Soc. Japan* **15**, 1994 (1960).

FIG. 1. Neutron total cross section for ^{16}O near the 3.770-MeV peak. The horizontal bars indicate the energy resolution, which was 5-keV full width at half-maximum for energies near the peak (open or closed circles) but 32 keV at other energies (open squares).



excitation energy and in width, to a ^{17}F state observed by ^{16}O proton scattering. However, the state in ^{17}F has been identified⁷ as $\frac{7}{2}^-$, whereas the ^{17}O state has a $J = \frac{5}{2}$ assignment.¹¹ In order to check this $\frac{5}{2}$ assignment, we have remeasured the total cross section of ^{16}O in the neighborhood of the 3.77-MeV peak with good energy resolution. We produced monoenergetic neutrons by bombarding zirconium-tritium targets with protons from the Oak Ridge National Laboratory's 5.5-MV Van de Graaff machine. In order to establish the proton energy scale, we located the thresholds of the $^3\text{H}(p,n)^3\text{He}$, the $^7\text{Li}(p,n)^7\text{Be}$, and the $^{19}\text{F}(p,n)^{19}\text{Ne}$ reactions with a long counter at 0° to the proton beam direction. Since the last reaction has a threshold $(4.2345 \pm 0.0009 \text{ keV})$ ²¹ very near the proton energy required to give 3.770-MeV $\text{T}(p,n)$ neutrons, we feel the absolute energy scale for our measurements is good to 3 keV. The energy resolution of our neutron beam was 5 keV full width at half-maximum for the measurements around 3.770 MeV. This we calculated from the shape of the neutron yield at the threshold of the $\text{T}(p,n)$ reaction which we measured with the long counter at 0° .

Our neutron detector for the total-cross-section measurements was a stilbene crystal (1 in. diam by $\frac{3}{8}$ in. long) located 55 cm in front of the neutron source. Pulses arising from γ rays were suppressed by pulse-shape discrimination.²² The sample, which was placed halfway between the source and the detector, was a 1.12-in.-diam by 1-in.-long beryllium-oxide cylinder which could be exchanged by remote control for a matching beryllium sample in order to subtract the

neutron transmission of the beryllium. A long counter at 90° to the neutron source served as the monitor. At each energy setting, we made a series of five counting measurements, three with the beryllium-oxide sample in place interspersed with two with the beryllium sample in place. We evaluated the room scattered neutron background by removing the direct source neutrons with a 32-cm-long Lucite rod between the source and the detector.

In Fig. 1 the open and closed circles show the results of two sets of measurements around 3.77 MeV made on different days with different zirconium-tritium targets of about the same thickness. The bars give typical counting errors. There is good agreement between the two sets of data. The cross sections have been corrected for room scattering background and for in-scattering. For this latter correction,²³ we used the 0° differential cross sections reported in this paper. The figure also shows off-resonance data, designated with squares, which we obtained by bombarding tritium in a gas cell to produce neutrons. The increased neutron intensity improved the statistics at the expense of energy resolution, which in this case was 32 keV full width at half-maximum. The very narrow resonance at 3.44 MeV gives only a slight increase in the cross section under this resolution.

The energy of the peak in Fig. 1 is $3.770 \pm 0.003 \text{ MeV}$, in agreement with Fossan *et al.*¹¹ The height is $2.30 \pm 0.20 \text{ b}$, and the full width at half-maximum is 20 keV. If we assume this is a single resonance then, correcting

²¹ A. Rytz, Nucl. Phys. **70**, 369 (1965).

²² F. D. Brooks, Nucl. Instr. Methods **4**, 151 (1959).

²³ D. W. Miller, in *Fast Neutron Physics*, edited by J. B. Marion and J. L. Fowler (Interscience Publishers, Inc., New York, 1963), Part II, p. 985.

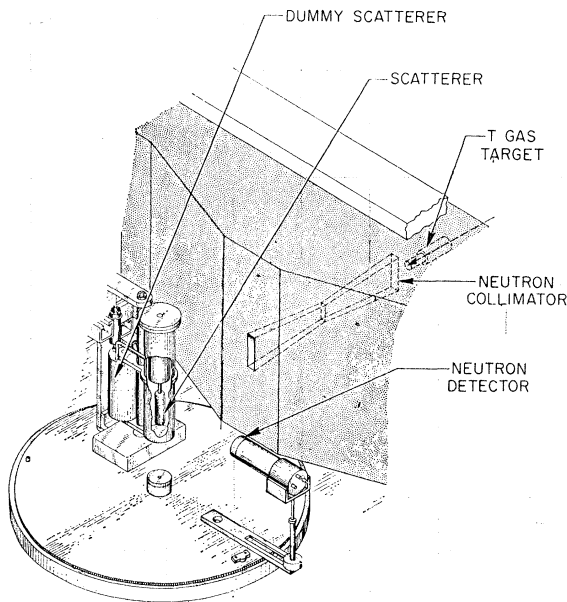


FIG. 2. Cutaway view of the neutron scattering chamber. Neutrons from the gas target enter through a tapered slot in the heavy front shield. The scatterer shown here is liquid oxygen in a thin-walled Dewar which can be exchanged by remote control for an empty "dummy" Dewar. The stilbene crystal detector can also be positioned by remote control.

for the experimental energy resolution of 5 keV, we find $\Gamma = 19$ keV, which is less than but consistent with the 22 keV reported by Walton *et al.*¹⁵ and the 25 keV found by Fossan *et al.*¹¹ Since the measured $^{18}\text{C}(\alpha, n)^{16}\text{O}$ cross section^{15,16} indicates the α width is negligibly small compared to the neutron width at 3.77 MeV, we expect a single resonance to have a peak height of 2.34 b if $J = \frac{5}{2}$ or 3.12 b if $J = \frac{7}{2}$. If we correct the observed peak height for energy resolution, assuming the resolution function is Gaussian, we find 2.39 ± 0.2 b for the resonant cross section, in good agreement with that expected for $J = \frac{5}{2}$.

We shall see in Sec. IV that the $J = \frac{5}{2}$ assignment is inconsistent with angular distributions and that the assumption that the 3.770-MeV peak is a single resonance is incorrect. In fact, we fit both the total cross section and the angular distributions under the assumption that there is a narrow, ~ 3 keV, $J = \frac{3}{2}^+$ resonance under an ~ 15 -keV $J = \frac{7}{2}^-$ resonance at 3.77 MeV. The large $d_{3/2}$ background phase shift makes the $\frac{3}{2}^+$ resonance appear as a dip under the $\frac{7}{2}^-$ resonance thus reducing its peak height in the total cross section.

III. DIFFERENTIAL CROSS SECTIONS

For the differential cross-section measurements, we used the neutron scattering chamber which was used previously²⁴ to determine the differential scattering from small ^{208}Pb samples with good energy resolution. Neutrons, collimated by a doubly tapered slot with a

1.2-cm \times 4.6-cm throat, were incident upon the sample which was supported in the center of a heavily shielded cavity 1 m square by 0.6 m deep. Figure 2 is a cutaway view of the chamber for the ^{16}O experiment showing the neutron source, collimator, scatterer, and detector.

Neutrons were produced by the $^3\text{H}(p, n)^3\text{He}$ reaction in a 3-cm-long gas cell containing tritium at about $\frac{1}{2}$ -atm pressure. We monitored the source with a long counter located outside the shielded region at a back angle to the proton beam. Several times during the experiment we measured the energy and the energy resolution of the neutron beam by measuring the transmission of the oxygen-scattering sample around the 3.77-MeV peak. We found that the 50- μ -in. nickel window of the cell introduced an energy spread of 22-keV full width at half-maximum.

The scatterer shown in the figure is a liquid-oxygen Dewar which was used for most of the work; however, for a preliminary set of angular distributions, we used beryllium-oxide and beryllium cylinders.²⁵ The beryllium-oxide sample was 4.5 in. long and 0.62 in. in diameter, and the dummy sample of beryllium contained the same weight of beryllium and was the same length as the beryllium-oxide sample.

Scattered neutrons were detected by the same stilbene crystal that was used in the total cross section measurements. Since the energy of the elastically scattered neutrons from ^{16}O decreases with increasing scattering angle, we must know the dependence of the efficiency on energy from the energy E_0 at 0° down to about $0.8E_0$. This information, over a slightly larger energy range, is also required for the multiple scattering correction. Therefore, we compared the relative efficiency of the crystal with that of a long counter in separate experiments before and after a series of angular-distribution measurements.

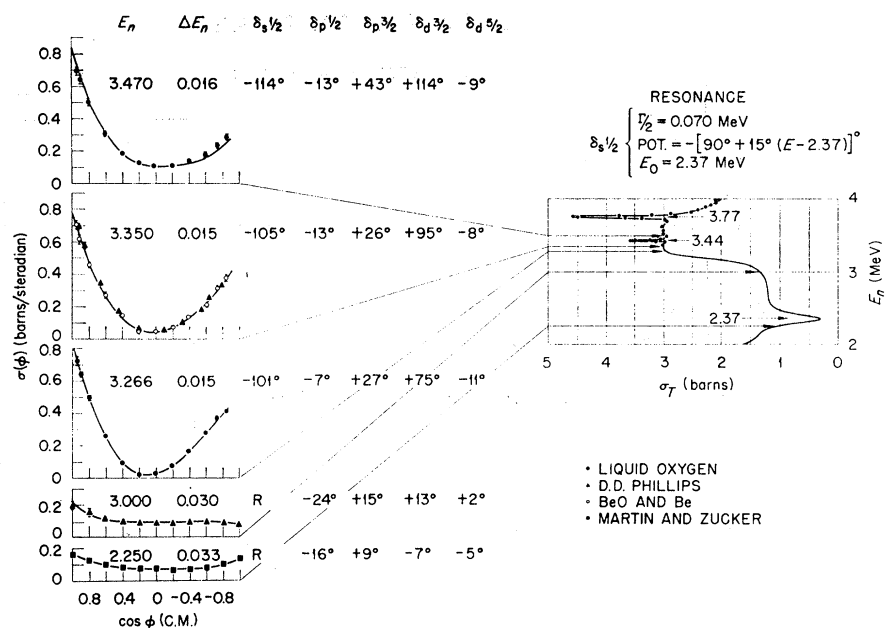
Both the samples and the detector could be moved and accurately positioned by remote control. As Fig. 2 shows, either the main sample or the dummy could be moved into position in the neutron beam, and the angular position of the detector could be changed by rotating the circular mounting table. In the process of lining up the apparatus, we measured the neutron transmission of the beryllium-oxide sample as a function of the angular position of the detector. This not only gave us the zero of the angle scale but also checked the alignment of the sample in the center of the collimated neutron beam. The spacings for the work with the beryllium-oxide sample were 87 cm between the centers of the source and the sample, and 15.5 cm between the centers of the sample and the detector.

For each angular measurement we followed a routine procedure in order to minimize possible errors due to drifts in detector efficiency. We first removed the samples from the beam and placed the detector at 0° in order to measure the direct flux relative to the counts

²⁴ J. L. Fowler, Phys. Rev. 147, 870 (1966).

²⁵ C. H. Johnson and J. L. Fowler, Bull. Am. Phys. Soc. 9, 348 (1964).

FIG. 3. Differential cross sections for E_n from 2.25 to 3.47 MeV. On the left are plots of the cross section $\sigma(\phi)$ versus $\cos\phi$ in the center-of-mass system. The data include not only the present work with either the beryllium-oxide (\circ) or liquid-oxygen (\bullet) scatterers, but also measurements by D. D. Phillips (\blacktriangle) and by Martin and Zucker (\blacksquare), quoted in Ref. 20). For each plot, values are shown for the neutron energy E_n , the energy resolution ΔE_n , and the phase shifts for the fit to the data. The letter "R" indicates that this particular phase shift was fixed by the parameters of the nearby resonance as indicated in the upper right-hand part of the figure. Also shown in the right of the figure is the total-cross-section curve from Ref. 11. The arrows from left to right indicate the point or energy of the total cross section at which the differential cross sections were measured.



in the fixed monitor. Next we rotated the crystal to the desired angle and recorded the counts with the beryllium-oxide sample, the beryllium sample, and a blank sample holder in the scattering position each for 10 times the monitor count of the 0° run. We then returned the counter to 0° for another measurement of the direct flux. We repeated this procedure for the other angles selected in a somewhat random fashion until we had accumulated about four measurements at each angle.

Since we effectively calibrated the neutron detector in the 0° beam, the measurements allow us to obtain absolute cross sections. Multiple scattering corrections were based on a procedure discussed in the literature for scattering from a cylindrical sample.²⁶ The method was altered to apply to neutrons scattered at resonant energies, as briefly described in a previous publication on beryllium-oxide and beryllium scattering.²⁷ With the sample of beryllium-oxide used here, the multiple scattering correction amounted to the order of 30% at angles where the cross section is low. We also corrected our results for self-attenuation, for the finite angular resolution, and for the energy dependence of the detector efficiency. We estimated the errors of the corrections as being $\frac{1}{3}$ the magnitude of the corrections and added these in quadrature to the standard errors of counting.

The resulting cross sections are included in Figs. 3 and 5. Here, as well as in Figs. 4 and 6, the plots on the left show the differential cross section versus the cosine of the scattering angle in the center of mass system. The neutron energy for each distribution is indicated.

²⁶ M. Walt, in *Fast Neutron Physics*, edited by J. B. Marion and J. L. Fowler (Interscience Publishers, Inc., New York, 1963), Part II, pp. 1033-1056.

²⁷ J. L. Fowler and H. O. Cohn, *Phys. Rev.* **109**, 89 (1958).

graphically by an arrow which connects to the total-cross-section curve on the right. These total cross sections are from Fossan *et al.*,¹¹ except for the curve in Fig. 5 which is from our own data in Fig. 1. The differential cross sections obtained with the beryllium-oxide and beryllium samples are shown as open circles with vertical bars to indicate the combined errors. At 3.35 MeV in Fig. 3, there is excellent agreement with the results of Phillips as quoted by Goldberg *et al.*²⁰

Because the multiple-scattering corrections were so large for the beryllium-oxide experiments, we replaced the scatterer with a very thin-walled Dewar flask containing liquid oxygen. This is shown in Fig. 2. The 0.001-in.-thick inner wall was of brass. The outer wall, which was under atmospheric pressure, was 0.01 in. of stainless steel; it had to be work-hardened to withstand the pressure. The dummy sample was an identical evacuated Dewar flask. The diameter of the liquid-oxygen container was $\frac{3}{4}$ in. and the length was about 4 in. It was supported by a $\frac{1}{4}$ -in.-diam tube which connected it with a liquid-oxygen reservoir which was above and outside of the neutron beam. The position of the neutron source and the geometry of the collimator determined the fraction of the connecting tube which was irradiated by the neutrons. Since the cross-sectional area of this tube was small compared to that of the sample container, the correction for the liquid in the tube was very small, about 1%. In order to determine the absolute cross section, we measured the mass of liquid oxygen contained in the Dewar flask by filling the flask and the $\frac{1}{4}$ -in. tube with liquid oxygen and collecting the oxygen gas as it evaporated into a glass cylinder with a closed end inverted over water. The mass found in this way was 33.9 g and is approximately 1% less

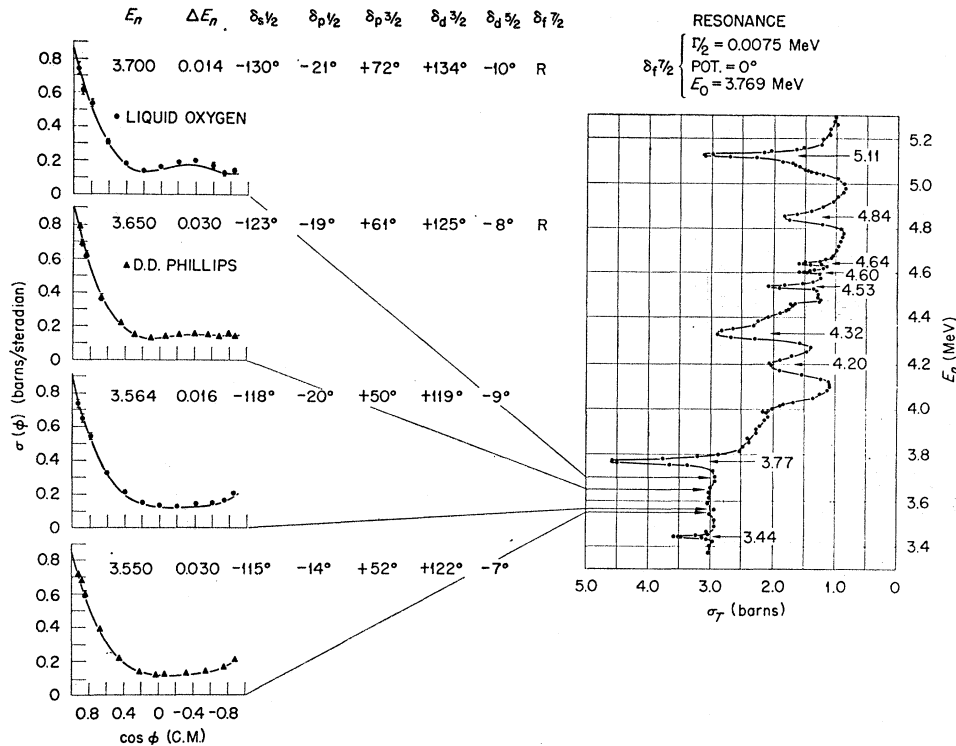


FIG. 4. Differential cross sections for E_n from 3.55 to 3.70 MeV. For details, see the caption for Fig. 3.

than that calculated from the volume of the container and the density of liquid oxygen. This discrepancy is consistent with the fact that the liquid oxygen contained some bubbles.

We had the Dewar flask x rayed before the experiment so that we could align the liquid-oxygen sample in the neutron beam. Then we checked the alignment in the same manner as for the beryllium-oxide sample by measuring the transmission of the liquid oxygen at the energy of the peak of the 3.77-MeV resonance.

For each angular measurement we used the same procedure as with the beryllium-oxide experiment except that we no longer needed to measure the beryllium background scattering. In Figs. 3–6, the data for scattering from liquid oxygen are denoted by closed circles. As in the case of beryllium-oxide scattering, we have corrected the data for the effects of spurious backgrounds, self-attenuation, multiple scattering, finite-angular resolution, and energy dependence of the detector efficiency. Here again we estimated the errors of the corrections as being $\frac{1}{3}$ the magnitude of the corrections and added these errors in quadrature with the standard counting errors. Since the sample was somewhat thinner than it was in the beryllium-oxide case, the multiple scattering corrections were reduced by a factor of 2. At 3.77 MeV (Fig. 5), there is agreement within the statistics between the data taken with the beryllium-oxide samples and those taken with liquid oxygen.

IV. ANALYSIS

The solid lines through the experimental differential cross section points in Figs. 3–6 are the results of least-squares phase-shift fits to the data with the phase shifts and resonance parameters listed in the figures. For most of the phase-shift analysis we used the Program ANNA²⁸ which had been developed to analyze the scattering of neutrons from ^{208}Pb and which was briefly described in a recent publication.²⁴ A subroutine of the program calculates differential cross sections for neutron scattering from 0-spin nuclei from a set of phase shifts, one of which must be taken from the parameters of a nearby resonance. The main program averages the theoretical cross sections from this subroutine over the energy spread of the measurements and uses matrix operations to adjust the nonresonant phase shifts in order to arrive at a minimum in the weighted squares of the deviations between the experimental points and the theoretical values. Thus for each angular distribution, all phase shifts were treated as independent variables except the one that is designated by R in each figure. For energies from 3.2 to 3.6 MeV, all of the important phase shifts were allowed to vary because there are no nearby dominant resonances; the formal requirements of the code were satisfied in this region by fixing the unimportant $f_{7/2}$ phase shift.

In our present analysis (which covers the energy

²⁸ Included in Brookhaven National Laboratory Report No. BNL-9108, 1965 (unpublished).

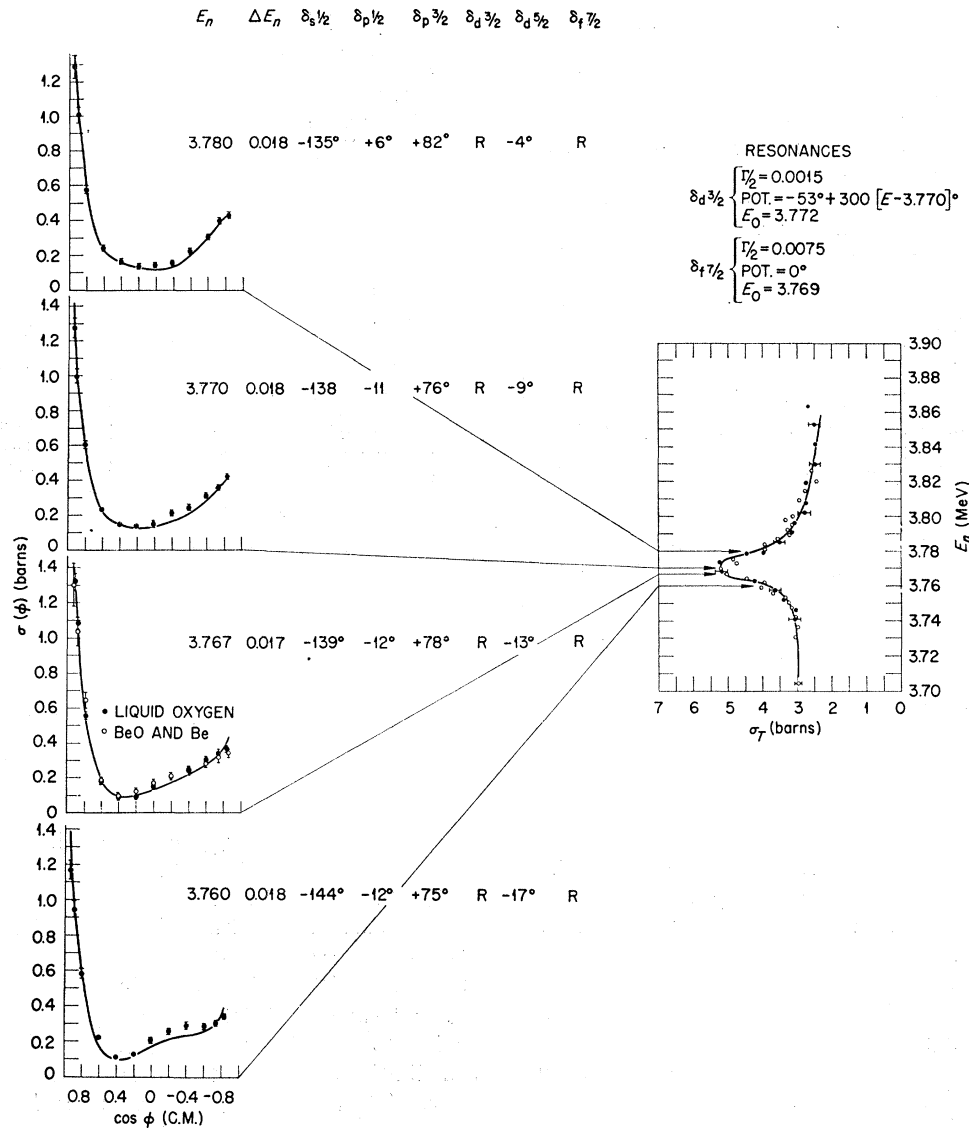


FIG. 5. Differential cross sections near the 3.770-MeV resonance. The details are the same as given in the caption for Fig. 3 except that all of the data here, both differential and total cross sections, are from the present work.

region from 2.25 to 4.20 MeV) we have included from the literature compilations²⁰ those neutron differential cross sections which had been obtained by detecting scattered neutrons. Angular distributions deduced from nuclear recoil energies are not included because they are unreliable or nonexistent at forward-scattering angles where the scattering cross sections change most rapidly with angle. As is well known, several sets of phase shifts can usually be found to fit a given angular distribution. Therefore, we required a smooth and consistent variation of the phase shifts with energy in order to select the sets listed in Figs. 3-6. For example, at 2.25 MeV, we began our fitting program with input phase shifts which, as Fig. 7 shows, are reasonable extrapolations from those known²⁷ at lower energies. The single fixed

phase shift was determined by the $s_{1/2}$ resonance at 2.37 MeV. The program then adjusted all but the $s_{1/2}$ input phase shifts to give a least-squares fit to the data. The analysis of the differential cross section at 3.55 MeV illustrates the difficulty in selecting a consistent set of phase shifts. In an earlier analysis we got an equally good fit to the data with a set of phase shifts in which $\delta s_{1/2} = -73^\circ$, $\delta p_{1/2} = -190^\circ$, $\delta p_{3/2} = +24^\circ$, $\delta d_{3/2} = +91^\circ$, and $\delta d_{5/2} = +2^\circ$. The set listed in Fig. 4, however, is much more consistent with the neighboring phase shifts as shown in Fig. 7.

In applying the test for smooth and consistent variations, it is desirable to have estimates of the experimental uncertainties in the phase shifts. However, these estimates are not trivial because the phase shifts

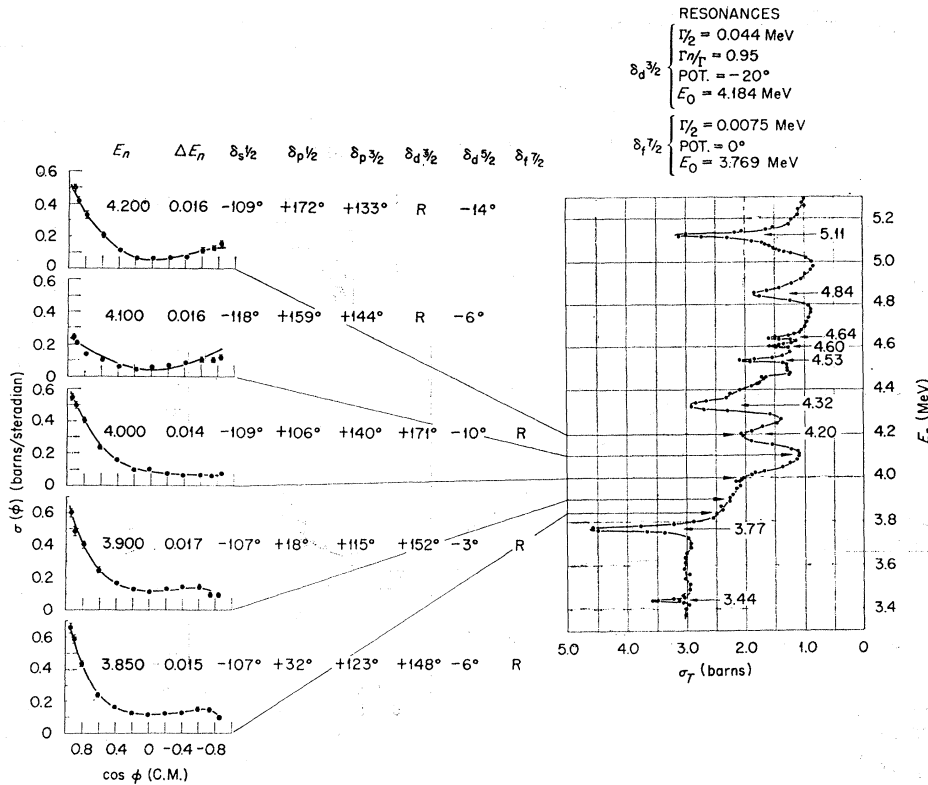


FIG. 6. Differential cross sections for E_n from 3.850 to 4.200 MeV. All of these differential cross sections were obtained with the liquid-oxygen scatterer but otherwise the caption for Fig. 3 gives the details.

are related in a complicated manner to the individually observed cross sections. Therefore, we used a method²⁹ in which we simulated several repeated experiments with artificially constructed data and then found the standard errors in the phase shifts for the best fits to these several experiments. In order to construct each artificial datum point, we treated the best-fit cross section in the figure as if it were the true value and then altered it by an increment chosen randomly from a distribution with the same standard deviation as the actual data point. Such an analysis gives an uncertainty for the phase shifts for the 3.00-MeV data of $\pm 2^\circ$. We show other phase-shift uncertainties with the vertical flags on selected values plotted in Fig. 7.

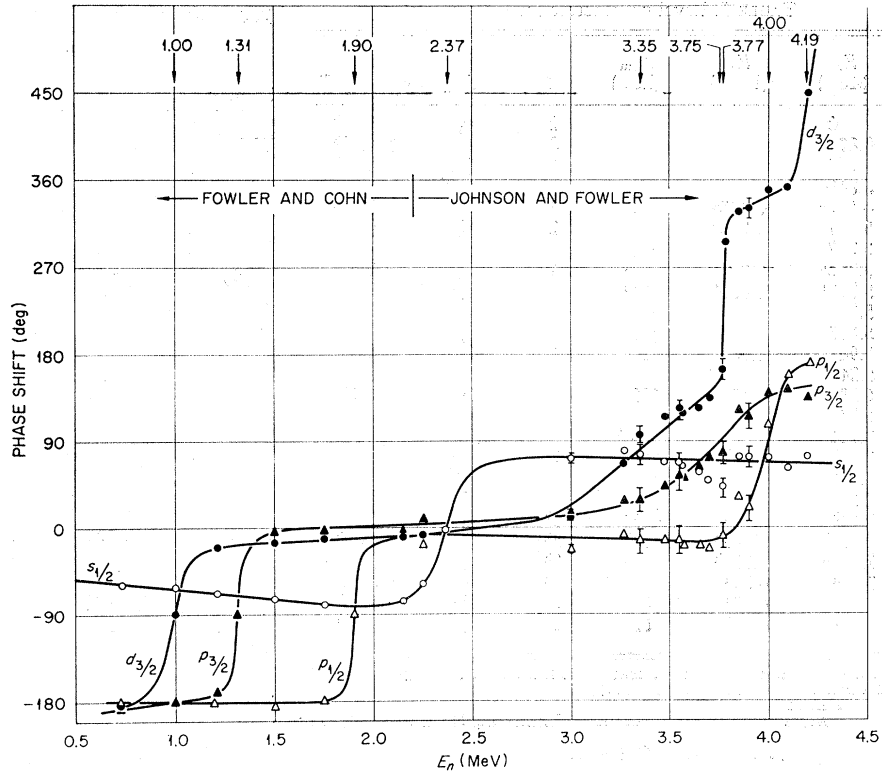
At the 3.77-MeV peak, Fig. 5, there has existed for a long time a serious difficulty in the analysis. As explained in Sec. II, the height and width are consistent with the identification of this peak as a single resonance with $J = \frac{5}{2}$. Indeed, the angular distribution at 3.77 MeV can be fitted under the assumption that it is a $\frac{5}{2}$ -resonance.¹⁸ As Lister and Sayres¹⁹ have pointed out, however, one cannot fit the angular distributions on either side of the resonance with a consistent set of phase shifts and a $\frac{5}{2}$ - or a $\frac{5}{2}$ + assignment. Figure 5 shows our solution for this problem. There is a narrow, 3-keV, $J = \frac{3}{2}$ + resonance under a 15-keV, $J = \frac{7}{2}$ -resonance. The large $d_{3/2}$ background phase shift, Fig.

7, makes the narrow $d_{3/2}$ resonance show up as a dip thus reducing the peak height in the total cross section. Incidentally, for the angular distributions shown in Fig. 4, particularly near 3.70 MeV, the tail of the 15-keV $f_{7/2}$ resonance at 3.77 MeV begins to influence the angular distributions and is included in the analysis.

For the analysis for the energy region shown in Fig. 5, we had to alter the fitting program so as to include the contributions of these two narrow overlapping resonances. The altered program calculates the phase shifts as a function of energy from assumed resonance parameters for each of these resonances. Using these phase shifts, the program adjusts the nonresonant phase shifts in the usual way. In order to obtain satisfactory fits to the angular distributions, we then vary in separate steps the assumed resonance parameters in such a manner that we adequately reproduce the total cross section (right-hand side of Fig. 5). As is evident in Fig. 5, the final selection of resonance parameters reproduces the total cross section quite well, and gives a reasonable fit to the angular distributions at energies in the neighborhood of 3.77 MeV with a consistent set of nonresonant phase shifts, Fig. 7. Attempts to make similar fits with a narrow $s_{1/2}$ resonance under the $\frac{7}{2}$ -peak were unsuccessful. For the mirror nucleus ^{17}F , as mentioned earlier, the resonance which corresponds both in excitation energy and in width to the 3.77-MeV peak has been identified as a $f_{7/2}$ resonance.⁷ Furthermore, in the phase-shift analysis of the proton scattering

²⁹ S. T. Thornton, C. H. Johnson, and J. L. Fowler, *Bull. Am. Phys. Soc.* **10**, 261 (1965).

FIG. 7. Phase shifts for $s_{1/2}$ through $d_{3/2}$ partial waves. The values below 2.25 MeV are from an earlier paper (Ref. 27) and the points above are from the present work, Figs. 3-6. The vertical bars are representative experimental uncertainties which are discussed in the text. Curves are drawn smoothly through the points. Resonance energies, i.e., energies at which phase shifts pass through 90° , are indicated at the top of the figure. Certain very narrow resonances of unknown partial waves, such as one at 3.44 MeV, are omitted from the figure.



from ^{16}O , a narrow $d_{3/2}$ resonance and a very narrow $s_{1/2}$ resonance show up in the vicinity of the $f_{7/2}$ state of ^{17}F .

Up to ~ 4.0 MeV the (n,α) cross section is negligible,^{15,16} so that we made the phase-shift analysis under the assumption of pure elastic scattering. At the 4.3-MeV peak, however, the α width is 5% of the total width.¹⁶ For the 4.1- and 4.2-MeV angular distributions, Fig. 6, we had to include in the fitting program the effect of the (n,α) competition with elastic scattering. Because of the interference of the resonant phase shift with the potential phase shift, the peak of the cross section at 4.2 MeV is shifted away from the resonant energy, which for the fits in Fig. 6 occurs at 4.184 MeV.

V. CONCLUSIONS

Figure 7 shows our $s_{1/2}$ through $d_{3/2}$ phase shifts as a function of neutron energy and includes results from a previous experiment.²⁷ Baldinger, Huber, and Proctor,¹⁷ in analyzing differential scattering data deduced from nuclear recoils, have given a set of phase shifts for the 2- to 4-MeV neutron energy range. Their $s_{1/2}$ and $p_{3/2}$ phase shifts are qualitatively in agreement with those shown in Fig. 7, and their $d_{3/2}$ phase shifts pass through 90° at ~ 3.4 MeV, as is the case in Fig. 7, but with a rate of change with energy about twice that shown in Fig. 7. Moreover, their $p_{1/2}$ phase shifts, which are positive where ours are negative, do not show the $p_{1/2}$

resonance at 4.0 MeV. Experiments on the $^{13}\text{C}(\alpha,n)^{16}\text{O}$ reaction¹²⁻¹⁶ have shown up a $J=\frac{1}{2}$ resonance at an excitation energy corresponding closely to 4.0-MeV neutron energy. Its width also corresponds closely to the slope of the $p_{1/2}$ phase shift at 4.0 MeV in Fig. 7.

A recent phase-shift analysis by Lister and Sayres,¹⁹ based on nuclear-recoil energy measurements, is in agreement with Fig. 7, in that the widths of the broad $p_{3/2}$ and $d_{3/2}$ resonances are around $\frac{1}{2}$ MeV. The $p_{1/2}$ phase shifts from this latter work, while negative up to ~ 3.7 MeV in fair agreement with our $p_{1/2}$ phase shifts, have too small a slope to correspond to the $p_{1/2}$ resonance at 4.0 MeV, and is thus in disagreement with our results as well as those of Walton *et al.*¹⁵ and Barnes *et al.*¹⁶ The $d_{3/2}$ phase shifts in the work of Lister and Sayres¹⁹ show the 4.18-MeV resonance in agreement with the phase-shift plot in Fig. 7. As pointed out earlier, their angular distributions revealed that the peak at 3.77 MeV could not be a $J=\frac{5}{2}$ resonance. Nevertheless, their analysis, based on a $J=\frac{7}{2}$ assumption for this peak, was inconsistent with the total cross section assignment of $J=\frac{5}{2}$ in the literature.¹¹ As discussed in the previous section, we attribute this difficulty to a narrow $d_{3/2}$ resonance under the 3.77-MeV peak. The effect of this latter resonance on the $d_{3/2}$ phase shift is, of course, not evident in the work of Lister and Sayres.¹⁹

Schiffer *et al.*¹⁴ and Walton *et al.*¹⁵ assign parameters for resonances at excitation energies corresponding to 4.0, 4.19, and 4.32 MeV (see Fig. 4, right-hand side) as

TABLE I. Level parameters for ¹⁷O states.^a

E_x (MeV)	E_n (MeV)	$\Gamma_{c.m.}$ (keV)	l	J	$\gamma^2/(\hbar^2/\mu a^2)$
0			2	$\frac{5}{2}^+$	0.43 ^b
0.871			0	$\frac{1}{2}^+$	>1.00 ^b
3.058			1	$\frac{1}{2}^-$	0.02 ^b
3.846			3	$\frac{3}{2}^-$	0.02 ^b
4.562 ^d	0.442 ^d	45 ^d	1	$\frac{1}{2}^-$	0.06 ^d
5.087 ^e	1.000 ^e	94 ^e	2	$\frac{3}{2}^-$	0.45 ^e
5.217		<8			
5.380 ^e	1.312 ^e	41 ^e	1	$\frac{3}{2}^-$	0.02 ^e
5.707 ^f	1.659 ^f	<6 ^f	3	$\frac{7}{2}^-$	0.13 ^g
5.729		<8			
5.867	1.830	<8		$\frac{3}{2}^-$	
5.94	1.90	26	1	$\frac{3}{2}^-$	0.01
6.24					
6.38	2.37	132	0	$\frac{1}{2}^+$	0.02
6.87					
7.161		2.7			
7.30 ^h	3.35 ^h	500 ^h	2 ^h	$\frac{3}{2}^+$	0.23 ^h
7.37 ⁱ	3.44 ⁱ	<2		$\frac{3}{2}^+$	
7.56		<4		$\frac{3}{2}^+$	
7.67 ^h	3.75 ^h	405 ^h	1 ^h	$\frac{3}{2}^+$	0.07 ^h
7.691 ^h	3.769 ^h	14 ^h	3 ^h	$\frac{3}{2}^+$	0.03 ^h
7.694 ^h	3.772 ^h	3 ^h	2 ^h	$\frac{3}{2}^+$	0.001 ^h
7.91 ^h	4.00 ^h	69 ⁱ	1 ^h	$\frac{3}{2}^+$	0.02 ^h
8.08 ^h	4.18 ^h	82 ^{i,j}	2 ^h	$\frac{3}{2}^+$	0.03 ^h
8.21 ⁱ	4.32 ⁱ	62 ^{i,j}	1 ^h	$\frac{3}{2}^+$	0.01 ^h

^a All entries not otherwise indicated are from F. Aizenberg-Selove and T. Lauritsen, Nucl. Phys. 11, 1 (1959).
^b See Ref. 31.
^c T. K. Alexander, C. Broude, and A. E. Litherland, Nucl. Phys. 53, 593 (1964).
^d A. Okazaki, Phys. Rev. 99, 55 (1955).
^e See Ref. 32.
^f R. O. Lane, A. S. Langsdorf, J. E. Monahan, and A. J. Elwyn, Ann. Phys. (N.Y.) 12, 135 (1961).
^g See Ref. 33.
^h Present data.
ⁱ See Ref. 11.
^j See Ref. 16.

$\frac{1}{2}^{\pm}$, $\frac{3}{2}^{\mp}$, and $\frac{5}{2}^{\pm}$, respectively, where the parities alternate according to either the upper or the lower sets of assignments. Since we show that the parity of the 4.0-MeV resonance is minus and that of the 4.10-MeV one is plus, all of these experiments together show that the 4.32-MeV resonance is $J = \frac{3}{2}^-$. This set of parity assignments for the three resonances also gives the best fit to the ¹³C(α, α) data of Barnes *et al.*¹⁶

In Table I we list all of the known bound and resonance states of ¹⁷O up through 8.19-MeV excitation energy together with estimates of their reduced widths in units of single particle widths. Following the procedure recommended by Vogt,³⁰ we have chosen a nuclear radius $a = 4.2$ F (fermis) such that a square well of this radius will give the experimental bound state and the s -wave phase shifts near zero energy.²⁷ In such a well, a single-particle s state has a reduced width of $\hbar^2/\mu a^2$, but the penetrability for the s -state is artificially reduced because of the reflection at the sharp boundary.³⁰ For higher angular momentum states, d states, for example, the penetrabilities are not so seriously affected. The 4.2 F radius used in the Wigner-Eisenbud resonance formalism gives a single-particle d state a width of ~ 200 keV at 1.0-MeV neutron energy. A

³⁰ E. Vogt, Rev. Mod. Phys. 34, 723 (1962).

Woods-Saxon potential well,

$$V = -V_0[1 + \exp(r - R_0)/b]^{-1},$$

with $b = 0.6$ F gives a width of ~ 180 keV for this d state, in rough agreement with the 200 keV. A value of 0.6 F for b is reasonable for the diffuseness parameter for nuclear potentials.

Below 4.146-MeV excitation energy the ¹⁷O states are bound. Here the relative reduced widths deduced from (d, p) stripping³¹ are normalized in Table I to the reduced width of the 5.087-MeV resonance state which has its reduced width calculated from neutron total-cross-section measurements.³² The same procedure was used to find the width of the unbound 5.707-MeV level from stripping data.³³ Since the relative reduced widths for stripping were obtained from the plane-wave theory, they are only expected to be reliable to an order of magnitude. Indeed, with the normalization we have used, the reduced width in single-particle units of the 0.871 MeV $s_{1/2}$ state becomes 1.53, which is clearly too high. The stripping data of Keller³¹ and of Yagi *et al.*³³ should certainly be reanalyzed with the more sophisticated stripping theories.

In our earlier discussion in connection with the 3.77-MeV peak, we compared our analysis with that of data from proton scattering from ¹⁶O which gives resonance parameters for the mirror nucleus ¹⁷F.^{6,7} With the solution of the difficulty of the 3.77-MeV peak, the agreement in the principal features between the phase-shift analysis of both neutron and proton scattering from ¹⁶O is, in general, satisfactory. For example, the prominent states at ¹⁷O excitation energies of 6.38, 7.30, 7.67, and 7.69 MeV have analogous states in ¹⁷F. Of course, in the case of both nuclei there are a number of unidentified states of small widths. Table I shows that roughly $\frac{1}{3}$ of the states in ¹⁷O up to an excitation energy of 8.21 MeV are not completely identified.

In recent years there have been at least two theoretical approaches to the explanation of the spectrum of mass-17 nuclei. On one hand there is the particle-hole approach in terms of shell-model states,^{2,3} and on the other there is the approach based on a cluster model.¹ The two-particle one-hole explanation of odd-parity states below 6 MeV has met with some success.³ As Table I indicates, however, the prominent states in ¹⁷O are of even parity. Since the pertinent hole states in ¹⁷O are of odd parity and the low-lying particle states are of even parity, there is essentially no hope of the two-particle one-hole excitations explaining even-parity states. Brown and Green² have described the low-lying even-parity states of ¹⁶O and ¹⁷O in terms of mixing of the usual states of the shell model with states obtained by exciting particles out of a deformed core. In their

³¹ E. L. Keller, Phys. Rev. 121, 820 (1960).
³² H. R. Striebel, S. E. Darden, and W. Haerberli, Nucl. Phys. 6, 188 (1958).
³³ K. Yagi, Y. Nakajima, K. Katori, Y. Awaya, and M. Fujioka, Nucl. Phys. 41, 584 (1964).

model the $\frac{1}{2}^+$ state in ^{17}O at 6.38 MeV and the $\frac{3}{2}^+$ state at 7.30 MeV are interpreted in terms of three-particle two-hole and five-particle four-hole excitations. Although this approach gives reasonable agreement with experiment, there are difficulties. For example, even though they carry the expansion to obtain core excitations in even numbers of particle and hole states through four-particle four-hole states, they find more terms must be included to obtain correct transition rates between states or to obtain the correct quadrupole moment of ^{17}O in its ground state. The approach¹ based on the cluster model has no trouble in giving these transition rates and the quadrupole moment correctly; moreover, it gives an adequate description of the position and widths of the states of ^{17}O below 5.2 MeV. The theoretical problem associated with the cluster model is that of finding its connection with the shell model which, because of its successful correlation of so many properties of nuclei, is generally believed to be the basic starting point for any description of nuclei. That there

is such a connection between the cluster model and the shell model has been recognized for a long time.³⁴ In a recent review paper, this connection is explored in some detail.³⁵

ACKNOWLEDGMENTS

We wish to acknowledge the assistance we had from Dr. J. A. Biggerstaff and R. P. Cumby who helped us in checking out the pulse-shape discriminator circuits, and that from Mrs. Eugene Patterson who altered the phase-shift computer program to fit the special cases arising in ^{16}O neutron scattering. We wish also to thank S. T. Thornton, R. L. Kernell, W. T. Newton, R. A. Robinson, and W. C. H. White who at various times helped us in taking data during the course of this experiment.

³⁴ J. K. Perring and T. H. R. Skyrme, Proc. Phys. Soc. (London) **69A**, 600 (1956).

³⁵ V. G. Neudachin and Yu. F. Smirnov, At. Ener. Rev. **3**, 157 (1965).

Fluctuations in Excitation Functions for $^{12}\text{C}(^{16}\text{O}, \alpha)^{24}\text{Mg}^\dagger$

M. L. HALBERT, F. E. DURHAM,* AND A. VAN DER WOUDE†

Oak Ridge National Laboratory, Oak Ridge, Tennessee

(Received 29 March 1967)

Cross sections were measured at five angles for alpha-particle groups from the reaction $^{12}\text{C}(^{16}\text{O}, \alpha)^{24}\text{Mg}$. The measurements were made with 40–50-keV resolution over energy intervals as long as 9.9 MeV (c.m.). The data provided large samples for fluctuation analyses over compound-nucleus excitation energies from about 25 to 35 MeV. The average coherence width, which is dominated by compound states with $J \sim 10$, was found to be about 118 keV. It does not vary significantly with exit channel, angle, or excitation energy in the compound nucleus. Most of the data are well represented by the simple Ericson–Brink–Stephen statistical model and show no significant direct-interaction component. A pronounced peak appearing in several of the excitation functions near 31.8-MeV bombarding energy is not consistent with this model.

I. INTRODUCTION

FOR a simplified stochastic model of the compound nucleus at high excitation energies, Ericson^{1,2} and Brink and Stephen³ have shown that interference among overlapping compound levels will cause cross sections to fluctuate rapidly as a function of energy. Statistical analysis of the deviations from average behavior enables one to determine certain average properties of the compound system that are difficult or impossible to obtain otherwise, for example, the width Γ of the compound states.

† Research sponsored by the U. S. Atomic Energy Commission under contract with the Union Carbide Corporation.

* Temporary employee from Tulane University; partial support received from Oak Ridge Associated Universities.

‡ On leave 1963–1965 from the University of Groningen, The Netherlands.

¹ T. Ericson, Phys. Rev. Letters **5**, 430 (1960).

² T. Ericson, Ann. Phys. (N. Y.) **23**, 390 (1963).

³ D. M. Brink and R. O. Stephen, Phys. Letters **5**, 77 (1963).

The present report describes measurements and statistical analyses of excitation functions for $^{12}\text{C}(^{16}\text{O}, \alpha)^{24}\text{Mg}$ for alpha-particle groups going to the low-lying levels of ^{24}Mg . The excitation energies of the ^{28}Si compound nucleus were in the range from 25.6 to 35.5 MeV. Data were taken at intervals of 43 keV (center-of-mass) with an energy resolution of 40–50 keV (c.m.). The excitation functions were obtained at five laboratory angles, nominally 0° , 20° , 69° , 149° , and 178° . Much more complete angular distributions were measured earlier at a number of energies; these are described in the following paper.⁴ Reference 4 also contains data taken with 15-keV resolution to check for narrower structure (none was found).

A summary of the excitation-function measurements is given in Table I. The alpha-particle groups studied

⁴ M. L. Halbert, F. E. Durham, C. D. Moak, and A. Zucker, following paper, Phys. Rev. **162**, 919 (1967).